

Quantum Annealing based Power Grid Partitioning for Parallel Simulation

Carsten Hartmann*[Ⓜ], Junjie Zhang*[†][Ⓜ], Carlos D. Gonzalez Calaza[§][†][Ⓜ], Thimo Pesch*[Ⓜ],
Kristel Michielsen[§][†][Ⓜ] and Andrea Benigni*[†][‡][Ⓜ] *Senior Member, IEEE*

* ICE-1: Energy Systems Engineering

§ Institute for Advanced Simulation, Jülich Supercomputing Centre
Forschungszentrum Jülich, 52425 Jülich, Germany

† RWTH Aachen University, 52056 Aachen, Germany

‡ JARA-Energy, Jülich 52425, Germany
{c.hartmann, a.benigni}@fz-juelich.de

Abstract—Graph partitioning has many applications in power systems from decentralized state estimation to parallel simulation. Focusing on parallel simulation, optimal grid partitioning minimizes the idle time caused by different simulation times for the sub-networks and their components and reduces the overhead required to simulate the cuts. Partitioning a graph into two parts such that, for example, the cut is minimal and the sub-graphs have equal size is an NP-hard problem. In this paper we show how optimal partitioning of a graph can be obtained using quantum annealing (QA). We show how to map the requirements for optimal splitting to a quadratic unconstrained binary optimization (QUBO) formulation and test the proposed formulation using a current D-Wave QPU. We show that the necessity to find an embedding of the QUBO on current D-Wave QPUs limits the problem size to under 200 buses and notably affects the time-to-solution. We finally discuss the implications on near-term implementation of QA in combination to traditional CPU or GPU based simulation.

Index Terms—Parallel algorithms, Power system simulation, Quantum theory, Graph theory

I. INTRODUCTION

With the transformation of the energy system towards renewable energies, the efforts required to model, simulate and control the system are steadily increasing. Whereas in the past a limited number of large power plants adjusted supply to demand, power balancing is increasingly characterized by a much larger number of smaller generation units, mostly based on fluctuating renewable energies, as well as more and more flexible consumers and prosumers. One way to manage the complexity of simulating and controlling these systems is to parallelize the problem by separating the overall system into smaller subsystems, which can then be solved on separate computing nodes. This network partitioning can also enable the use of flexible, distributed and adaptable smart grids monitoring [1] and control solutions [2]. Other grid partitioning applications include dividing into optimal balancing regions to reduce i.e. administrative and computational complexity and loop flows [3]; controlled islanding to prevent failure spreading [4] and diakoptics based state estimation [1]. In this paper we focus on the problem of partitioning a power system graph so to enable parallel simulation. While dependent on the specific simulation algorithm used, in general [5]–[7], an

optimal partitioning for parallel simulation should ensure a good balancing of the computing loads and should minimize the overheads created by the partitioning.

The problem of grid or graph partitioning, in two or more parts, is a fundamental problem in computer science and combinatorial optimization, known for its NP-hard complexity [8], which is hard to solve for classical computers and heuristics are usually applied [9]. Consequently, recent advances in quantum hardware have raised interest in exploring the potential of quantum computation as an alternative to established classical approaches. Thus, a new research field is emerging: Quantum computation for power systems [10], [11]. Recent advances in this field can be grouped into three categories:

First, classical algorithms to solve systems of linear or nonlinear equations are replaced with quantum subroutines such as the HHL algorithm [12] or specially designed variational quantum circuits [13]. The HHL algorithm promises an exponential speed-up in the asymptotic limit if the problem is sparse [12] and the condition number can be bounded tightly [14]; however, it still faces input/output problems and requires circuits that are too deep for NISQ hardware. Nevertheless, proposed applications for HHL involve i.e. to solve DC and AC power flow equations [15], [16]. To circumvent some issues with the HHL algorithm, a variational circuit for a quantum electromagnetic transients program has been proposed [17]; however, quantum advantage has yet not been experimentally realized for any variational approach [13].

Second, decision problems representing fundamental operational or planning problems in power systems are reformulated to fit quantum optimization approaches. These involve the unit commitment problem [18], network reconfiguration in distribution grids [19] or optimal power flow [20]. However, on current hardware, only small problems can be tackled, which spiked recent interest in the decomposition of UC problem into smaller instances [21], [22].

Third, quantum optimization is used to support classical simulation or optimization by, e.g., finding optimal cut in benders decomposition to solve large instances for the UC problem [23].

The idea presented in this paper falls into the third category and explores graph partitioning to enhance the parallel simula-

tion of power systems. The graph partitioning problem entails dividing the vertices of a graph into subgraphs while minimizing the number of edges between different subgraphs and/or achieving other specific objectives. Partitioning a graph into two parts, such that both subgraphs are of equal size, admits a natural quadratic unconstrained binary optimization (QUBO) formulation [24]. Thus, the problem fits established quantum optimization paradigms such as quantum annealing (QA) [25] or QAOA [26]. If advances in hardware are achievable, both approaches promise to solve large problem instances that are classically intractable. Partitioning into more than two parts based on the idea of network modularity can also be mapped to a QUBO; however, it requires costly integer encoding [27].

The article is structured as follows: Section II gives a short overview of QA. Section III reviews, combines and extends QUBO formulations for graph partitioning. Section IV gives a short overview of parallel simulation of power grids and its relation to graph partitioning, considering the specific algorithm of [5]. Section V combines the findings of the previous two sections to derive a tailored graph partitioning QUBO for parallel simulation. Section VI discusses the optimal and near-optimal solutions and current hardware limitations.

II. SOLVING QUBOS USING QUANTUM ANNEALING

A. Quantum Annealing in a Nutshell

A quadratic unconstrained binary optimization (QUBO) problem in its general form is given by

$$\min_{\{z_n \in \{0,1\}\}} Q \quad (1)$$

$$Q = \sum_{n,m=1}^M z_n Q_{n,m} z_m,$$

where $Q_{n,m}$ are the entries of an $M \times M$ symmetric matrix. The objective function of a QUBO can be transformed into a classical Ising Hamiltonian H_P by a linear transformation in the variables $s_n = 2z_n - 1 \in \{-1, 1\}$. H_P is then the energy function of a spin glass, and the problem of finding an optimal solution of Q has been translated into finding a ground state of H_P . Due to symmetries in the problem, the ground state energy can be degenerate and several ground states encode equivalent solutions.

The idea of QA [25] is based on the quantum adiabatic theorem [28], [29] that roughly states that a closed system stays in its ground state if it undergoes an adiabatic transformation, that is a transformation that takes significantly longer than the time scales set by the internal dynamics. In quantum annealing, a system is initially prepared in a ground state of a mixer Hamiltonian H_M . Then the instantaneous Hamiltonian is 'slowly' evolved towards the problem Hamiltonian H_P in an *annealing schedule* given by

$$H(t) = A(t)H_M + B(t)H_P, \quad (2)$$

with: $A(0) \gg B(0)$, $A(T_A) \ll B(T_A)$,

where the tunneling energy A and problem energy B are monotonous functions whose typical schedule can be found in [30] and T_A is the *annealing time*, which should be large compared to the inverse of the minimum energy gap [31],

i.e. the energy difference between the ground state and the first excited state at the point of the evolution where these are closest in energy.

For current D-Wave Advantage QPUs, the mixer H_M is fixed as $\sum_n \sigma_n^{(1)}$ [30], [32]. Then, the ground state of H_M , thus the initial state, is given by the uniform superposition of all possible configurations in the eigenbasis of H_P . During anneal, H_M causes quantum tunneling between configurations in analogy to thermal fluctuations in simulated annealing [33]. After the anneal, the state of the spin glass is measured in the eigenbasis of H_P . In an ideal QA process, using a sufficiently large annealing time, the outcome $s_1 \dots s_N$ of this measurement should be one of the ground states of H_P .

Quantum annealing is a *heuristic* solver as the adiabatic theorem does not strictly apply in practice. The real-world implementation is neither closed nor are the annealing times infinitely long. Consequently, the system can undergo a transition to an excited state of H_P during anneal at any time, for example, due to thermal fluctuations. Then the outcome of an anneal is not a globally optimal solution to the original problem Q .

B. Assessing the Quality of a Solution

Since QA is a heuristic solver, similar to simulated annealing, one usually performs N_s anneals Eq. (2) to create N_s solution candidates. For each sampled configuration with energy $E_{sampled}$, the relative error is defined as

$$L = \frac{|E_{min, global} - E_{sampled}|}{|E_{min, global}|}, \quad (3)$$

where $E_{min, global}$ is the energy of the global optimal solution. In general, $E_{min, global}$ is not known a priori, except for two cases: The problem instance is small enough to be solved by brute force methods on CPUs, or the problem is formulated in such a way that the minimal energy of the objective function is known, cf., for example, the number partitioning problem discussed in [24].

To quantify the quality of a sample set, one defines the *lowest relative error* [34] as

$$L_{min} := \min_{E_{sampled}} L. \quad (4)$$

C. Time to (Best) Solution

As a consequence of sampling N_s times, the annealing time T_A is not the only parameter that affects the time to find a globally (or near) optimal solution, and there is a trade-off between longer annealing times and sampling more configurations. This trade-off is captured by the *time to solution (TTS)* [34], [35] which is defined as the 'time' to reach a globally optimal (or best) solution, at least once with probability p_S and is given by

$$TTS(p_S, T_A) := \frac{\log(1 - p_S)}{\log(1 - \frac{N_{opt}}{N_s})} T_A, \quad (5)$$

where N_{opt} is the number of globally optimal (or: best) solutions in the sample set.

The time to solution only partially reflects the actual QPU access time [36], as it only considers the annealing time and

neglects delays and constant-overhead QPU programming and readout times.

D. Minor Embeddings

The current D-Wave Advantage system has more than 5000 qubits and more than 35000 couplers [34] arranged in a Pegasus graph, in which qubits are coupled to at most 15 other qubits. To sample the QUBO on the QPU, the *logical graph* representing the couplings $Q_{n,m}$ between the variables z_n and z_m must be mapped to the hardware graph. If the QUBO can not be mapped directly, for example, due to the QUBO graph having a higher degree than that of the hardware graph, several physical qubits are strongly coupled ferromagnetically to form a *chain* representing one logical variable (or qubit) [37]. Finding such a (*minor*) *embedding* of the logical graph onto the QPU graph is usually done heuristically [38].

III. QUBO FORMULATION FOR GRAPH PARTITIONING

A *partition* of a graph $\mathcal{G} = (\mathcal{V}, \mathcal{E})$, where \mathcal{V} is a set of vertices/nodes and $\mathcal{E} \subseteq \mathcal{V} \times \mathcal{V}$ a set of edges connecting the nodes, is an allocation of nodes to two (or more) sub-graphs $\mathcal{G}_i = (\mathcal{V}_i, \mathcal{E}_i) \subset \mathcal{G}$ such that each vertex $v \in \mathcal{V}$ is in only one sub-graph. That is, the vertex sets \mathcal{V}_i are mutually disjoint and the union of all vertex sets is the original vertex set. The *cut* set is comprised by all edges $e = (v_i, v_j)$ that connect nodes $v_i \in \mathcal{V}_i$ and $v_j \in \mathcal{V}_j$ in different parts, that is, $i \neq j$. In this work, we primarily focus on the partitioning into two parts as this admits a straightforward binary representation of the problem.

Graph partitioning is a task frequently encountered in real-world applications, e.g. community detection [39], studying immunization strategies [40], and decomposition of quadratic pseudo-Boolean functions [41]. However, graph partitioning is known to be NP-hard [8]. Dedicated heuristics exist to find the optimal partitioning based on the goals of the application [42], in particular for power grids [9].

For the partitioning of a graph into two parts, another approach is to formulate the goals as objectives of a QUBO. The $N = |\mathcal{V}|$ binary/decision variables z_n encode to which part (sub-graph after partitioning) the n -th node belongs, that is

$$z_n = \begin{cases} 1 & \text{if node } n \in \mathcal{V}_1, \\ 0 & \text{if node } n \in \mathcal{V}_2. \end{cases} \quad (6)$$

Following the work of [24] and [39], we briefly review and extend QUBO formulations for four different objectives: Minimizing the cut [24], and balancing the sizes $N_i = |\mathcal{V}_i|$ of the two sub-graphs \mathcal{V}_1 and \mathcal{V}_2 [24], balancing the sum of the edge weights within both parts and maximizing the network modularity [39].

A. QUBO Formulations for the Single Objectives

1) *Minimal (Weighted) Cut*: One potential objective is to minimize the number of edges between both parts. A QUBO formulation for this goal has been derived by Lucas [24]. Here we extend Lucas's formulation to find the minimal *weighted* cut, a problem that is also associated with finding the maximal

flow [43]. Let $w_{n,m}$ be the weight associated with the edge $e = (n, m)$. We seek to minimize the sum of the weights over all edges in the cut set

$$Q_{cut} = \sum_{(n,m) \in \mathcal{E}} w_{n,m} (-2z_n z_m + z_n + z_m). \quad (7)$$

Note that $(-2z_n z_m + z_n + z_m) = 1$ if nodes n and m are in different sub-graphs and evaluates to 0 if they are in the same part.

Using the adjacency matrix \mathbf{A} of the graph \mathcal{G} , we can rewrite Eq. (7) as

$$Q_{cut} = \sum_{n,m \in \mathcal{V}} z_n (-2A_{n,m} w_{n,m}) z_m + \sum_{n \in \mathcal{V}} z_n \left(2 \sum_{m \in \mathcal{V}} A_{n,m} w_{n,m} \right) z_n, \quad (8)$$

to resemble the standard form (1) and read off the matrix elements $(Q_{cut})_{n,m}$.

2) *Balancing the Sizes of the Sub-Graphs*: Another potential goal is to balance between the sizes, i.e., the number of nodes N_i , of both sub-graphs. To derive the objective function in QUBO form given by Lucas [24], we start with the hard constraint that is satisfied if both sides have the same number of nodes

$$\sum_n z_n = \sum_n (1 - z_n).$$

By squaring the difference between both sides, we turn the hard constraint into a quadratic objective function

$$Q_{size} = \left(\sum_n z_n + \sum_n (z_n - 1) \right)^2, \quad (9)$$

that penalizes a partitioning if $N_1 \neq N_2$. By multiplying out, Q_{size} can be brought into the standard QUBO form, cf. Eq. (1).

3) *Balancing the Sum of the Edge Weights*: Instead of balancing the size of the sub-graphs, we could also seek to balance the sums of the edge weights $w_{n,m}$ (to the power p) between the sub-graphs. As a hard constraint, this can be written as

$$\sum_{n \in \mathcal{V}} \underbrace{\left(\sum_{m \in \mathcal{V}} A_{n,m} w_{n,m}^p \right)}_{:=\alpha(n,p)} z_n = \sum_{n \in \mathcal{V}} \alpha(n,p) (1 - z_n), \quad (10)$$

where we have introduced the term $\alpha(n,p)$ to shorten the notation. Again, this constraint can be turned into a quadratic objective function $Q_{weights}(p)$ by the same steps as for Q_{size} . Note that the weights of the edges in the cut set are attributed to both parts and thus cancel each other out. The power p can be used to tune the objective. If $p = 1$, the sums of all weights in each part are balanced. For $p \gg 1$, the contributions of small weights are scaled down relatively to the maximal weights, such that balancing the maximal weights is emphasized.

4) *Network Modularity*: Lastly, maximizing the network modularity [39] is a common method to detect communities, that is, highly connected components representing functional units. These components provide a natural partitioning of the graph. The (negative) network modularity is equivalent to an Ising Hamiltonian and, thus, admits a straightforward QUBO formulation given by

$$Q_{mod} = \sum_{n,m} z_n \left(\frac{-1}{M} (A_{n,m} - \frac{deg(n)deg(m)}{2M}) \right) z_m, \quad (11)$$

where M is the number of edges, $deg(n)$ the degree of node n . To derive Q_{mod} from [39] we have used that $\sum_m A_{n,m} = deg(n)$ and $\sum_n deg(n) = 2M$.

Graph partitioning into more than two parts using integer encoding based on the idea of network modularity has been recently discussed by Wang et al. [27].

B. QUBO using Linear Scalarization

Combining several of the previously introduced objectives, we obtain a *multi-objective optimization* program with potentially *conflicting objectives*. For example, Q_{cut} is minimized if the cut set is empty; that is, all nodes are allocated to the same part. However, this is not optimal if we also want to, e.g., balance the sizes of the two sub-graphs.

For quantum optimization, we need to turn the multi-objective optimization program into a single QUBO. Hence, we collect the single objectives in a weighted sum

$$Q = \sum_i \lambda_i Q_i, \quad (12)$$

where $i \in \{cut, size, weights, mod\}$.

The coefficients λ_i have to be chosen a priori and effectively determine the importance of each objective as they set the energy scale. Different choices for the coefficients λ_i can lead to different optimal points on the convex hull of the Pareto front [44].

IV. PARALLEL SIMULATION OF POWER GRIDS BASED ON NETWORK PARTITIONING

Parallel simulation of power networks following partitioning has been a common technique in power system simulations for decades. There are different but similar approaches proposed for parallel simulation with partitioned networks, which all involve simulating the partitioned sub-networks in parallel with a sequential part left associated with the link between the sub-networks [5], [45], [46]. Take the diakoptics-based method MATE [5] as an example. The modified nodal analysis (MNA) formulation of the electric network $YV = I$ for a partitioned network assumes a block diagonal form

$$\begin{bmatrix} \begin{bmatrix} Y_{N1} & 0 \\ 0 & Y_{N2} \end{bmatrix} & C \\ C^T & -Z_L \end{bmatrix} \begin{bmatrix} v_{N1} \\ v_{N2} \\ i_L \end{bmatrix} = \begin{bmatrix} h_{N1} \\ h_{N2} \\ -V_L \end{bmatrix}, \quad (13)$$

where h_{Nk} , Y_{Nk} , v_{Nk} for $k \in \{1, 2\}$ represent current injections, admittance matrix, nodal voltages (including currents chosen as independent variables as of MNA) in each sub-networks, respectively. C represents the connectivity matrix

of the link between partitions (referred to as "cut" in the following), and Z_L , i_L , V_L are the impedance matrix, current and voltage vectors over the cut, respectively. Reformulating Eq. (13) as

$$\begin{bmatrix} 1 & 0 & Y_{N1}^{-1}C_{N1} \\ 0 & 1 & Y_{N2}^{-1}C_{N2} \\ 0 & 0 & C_{N1}^T C_{N2}^T + Z_L \end{bmatrix} \begin{bmatrix} v_{N1} \\ v_{N2} \\ i_L \end{bmatrix} = \begin{bmatrix} Y_{N1}^{-1}h_{N1} \\ Y_{N2}^{-1}h_{N2} \\ Y_{N1}h_{N1} + Y_{N2}h_{N2} + V_L \end{bmatrix}, \quad (14)$$

shows that the solutions of each sub-network become independent of each other except for the cut. Hence, parallel computation of the sub-networks is possible after solving the equations over the cut. Additionally, finer parallelizations can be applied to each sub-network, such as the approaches in [6], [7], [47], [48]. Overall, each time step in simulating a partitioned network can be divided into three stages [5]:

- 1) Components of each sub-network are solved to obtain the injections to the network,
- 2) Equations over the cut are solved,
- 3) The network equations in each sub-network are solved in parallel with the injections from components and the cut.

Based on these three steps, we can formulate an optimization problem to find good partitioning so that the overall computation time is minimized. The objectives for optimal partitioning are:

- 1) minimizing the additional computational cost due to the cut,
- 2) minimizing the difference in computational cost among sub-networks to minimize the 'idle time'.

V. GRID PARTITIONING TO MINIMIZE OVERHEAD IN PARALLEL SIMULATION

A. Estimation and Balancing of Computational Costs

We now need to estimate the computational costs of simulating the partitioned sub-networks to derive the objective function. For simplicity, we approximate these costs using the computation needed number of floating point operations (FLOPs).

1) *Component costs*: Dynamic components can be described as differential algebraic system of equations (DAE) and solved with numerical integration. Assuming explicit methods are used, we can discretize the integration as

$$x_{k+1} \leftarrow x_k + h\dot{x}_k, \quad (15)$$

$$y \leftarrow g(x), \quad (16)$$

where Eq. (15) describes the integration of internal states x, y of the component and Eq. (16) the injections from components to the grid. Therefore, we take the FLOPs in computing Eq. (15), Eq. (16) to represent the cost c_i for solving the i^{th} component.

A partitioning of the network into two sub-networks decomposes all components into three disjoint sets: the sets of all components in distinct parts (sub-network 1, 2), and in the cut, respectively. Let $C_{1(2)}$ and C_{cut} be the index sets, e.g.

the i^{th} component is in part 1 if $i \in C_1$. Then the 'idle time', i. e. mismatch of computing load in different sub-networks, is given by

$$\Delta W_{comp.} = \sum_{i \in C_1} c_i - \sum_{i \in C_2} c_i. \quad (17)$$

2) *Cut costs*: Computations on the cut consist of two parts, updating the mutual injections between the cut and sub-networks and solving the component equations and network equations within the cuts. Since the computation for updating the injections are matrix-vector multiplications, the cost for solving the component equations and updating the injections for two sub-networks is given by

$$W_{cinj} = \sum_{i \in C_{cut}} c_i + 4M_c(N-1) + M_c,$$

where M_c is the number of edges in the cut.

Solving for the cut or the sub-networks (see below) is equivalent to solving independent sets of linear equations, i. e. solving $Ax = b$ for x . We assume that LU decomposition is used since the decomposition must only be performed once if there are no topological changes. In each simulation step, the cost for solving the (sub)-network is then given by the FLOPs for forward and backward substitution. Hence, for solving the network equations over the cut, we have

$$W_{cut, network} = 2M_c^2 - M_c.$$

Using that $M_c \ll N$, the total overhead induced by the cut can be estimated as

$$W_{cut} \approx \sum_{i \in C_{cut}} c_i + 4(N-1)M_c. \quad (18)$$

3) *Sub-network costs*: Solving for the sub-networks is again done by LU decomposition. Therefore, the mismatch in solving sub-network is given by the difference between forward and backward substitution costs in each part:

$$\begin{aligned} \Delta W_{networks} &= 2(N_1^2 - N_2^2) - (N_1 - N_2) \\ &= 2N\Delta N - \Delta N. \end{aligned} \quad (19)$$

B. Graph representation

Let $\mathcal{G}_{grid} = (\mathcal{V}_{grid}, \mathcal{E}_{grid})$ be a graph representing the grid topology, that is, the nodes $n \in \mathcal{V}_{grid}$ represent buses and the edges $e \in \mathcal{E}_{grid}$ represent the electrical transmission lines. To put all the components, i. e. generators and transmission lines, on an equal footing, we construct a *simulation graph* $\mathcal{G}_{sim} = (\mathcal{V}_{sim}, \mathcal{E}_{sim}) \supset \mathcal{G}_{grid}$ based on the grid \mathcal{G}_{grid} in the following way: Except the transmission lines that are already represented as edges, we represent each component attached to a bus $n \in \mathcal{V}_{grid}$ by an *additionally added edge*¹ that is incident to the bus n . Hence all electrical components are represented by edges in the graph \mathcal{G}_{sim} . To all edges, we then assign a weight $\hat{c}_e = c_e/c_{max} \in [0, 1]$ that represents the normalized computational cost (normalized FLOPs) of simulating the respective component, cf. Section V-A. The steps to construct \mathcal{G}_{sim} are illustrated in Fig. 1.

¹We also add an additional node for each component.

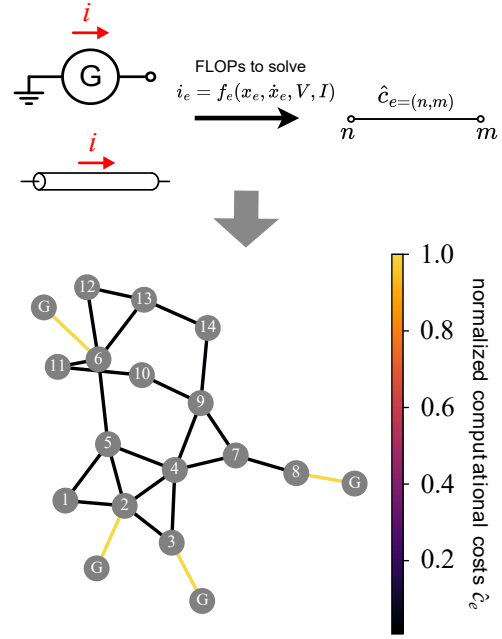


Fig. 1. Steps to turn power grid into \mathcal{G}_{sim} . First, map each component, e.g. generator and lines, to an edge e whose weight \hat{c}_e represents the FLOPs needed to solve for the current i_e . Second, build a graph that resembles the grid topology.

The problem of finding an optimal partitioning of the network into two sub-networks for parallel simulation is thus equivalent to finding an optimal partitioning of the graph \mathcal{G}_{grid} taking into account all components whose computational costs are represented by the weights c_e of the edges in \mathcal{G}_{sim} . We only need to partition the graph $\mathcal{G}_{grid} \subset \mathcal{G}_{sim}$ as the nodes in $\mathcal{V}_{sim} \setminus \mathcal{V}_{grid}$ don't represent any additional partition choices regarding the network and thus the components: All edges representing components between nodes in different parts \mathcal{V}_i are in the cut set. For all other components, there is at least one node $n \in \mathcal{V}_{grid}$ incident whose assignment to \mathcal{V}_1 or \mathcal{V}_2 provides the assignment of the component to part 1 or part 2.

C. QUBO Formulation

To find an optimal partitioning of \mathcal{G}_{grid} we map each of the three objectives of minimizing the costs for simulating the cut, balancing the cost of simulating the costs and the network in each part, see section IV, to one of the general QUBO objectives from section III. Each of these mappings is chosen such that the objective values of the QUBO term are some measure for the computational overhead that arises due to the partitioning into sub-networks, cf. section V-A. The sum of all three objective values is then an estimate for the quality of the partitioning and the full QUBO objective function is thus a simple sum of three terms

$$Q_{part.} = Q_{components} + Q_{cut} + Q_{network}. \quad (20)$$

Due to this construction, we avoid the additional problem of choosing the weights λ_i a priori.

1) *Reduce 'idle' time in component simulation*: For the component simulation step, we want to minimize the idle time

that arises if one part can be simulated faster than the other, see Eq. (17). By adopting from $Q_{weights}$ in Eq. (10), a QUBO objective function $Q_{components}$ that computes the squared idle time for a given partitioning is given by

$$Q_{components} = \sum_{n,m \in \mathcal{V}_{grid}} z_n (4\alpha(n)\alpha(m)) z_m + \sum_{n \in \mathcal{V}_{grid}} z_n (-4\alpha(n)\beta) z_n + \beta^2, \quad (21)$$

where $\alpha(n) := \sum_{m \in \mathcal{V}_{sim}} A_{n,m}(\mathcal{G}_{sim}) \hat{c}_{n,m}$ and $\beta = \sum_{m \in \mathcal{V}_{grid}} \alpha(m)$.

2) *Minimize the computational costs of cut simulation:* Minimizing the total overhead due to the cut simulation can be mapped to finding a weighted minimal cut. We have already introduced a QUBO Q_{cut} formulation for weighted minimal cuts in Eq. (8). To incorporate the costs for the component and network simulation of the cut and compute the overhead according to Eq. (18), we define the edge weights $w_{n,m}$ as

$$w_{n,m} = \hat{c}_{n,m} + 4 \frac{N-1}{c_{max}}, \quad (22)$$

for the edges in \mathcal{G}_{grid} . We normalize the costs attributed to the network and the injections by c_{max} to obtain normalized flops.

3) *Reduce 'idle' time in network simulation:* For the parallel network simulation step of the sub-networks, both parts should have the same size (=number of nodes) to reduce the idle time given by Eq. (19). We thus scale Q_{size} in Eq. (9) as

$$Q_{network} = \frac{(2N-1)^2}{c_{max}^2} Q_{size} \quad (23)$$

in order to calculate the squared idle time.

D. Partitioning for more than two computational nodes

Suppose we seek to partition the grid into P parts. In that case, a direct approach is to define integer variables $z_n \in \{0, 1, \dots, P-1\}$ to encode the partitioning and then extend the QUBO objectives to the more general case. However, encoding integer variables into binary variables significantly increases the complexity, in particular, the number of qubits. Hence, even small problem instances become impossible to embed and solve on near-term hardware.

If we seek to distribute the computation to $P = 2^n$ workers, another approach is to partition the (sub-)networks into two parts iteratively. However, an iterative approach does not guarantee a globally optimal result. The difference between an iterative quantum optimization approach and the mixed integer programming approach introduced above is a research question that we intend to investigate in the near future.

E. Ensuring Connectedness

The derived QUBO objective function $Q_{part.}$ does not enforce that each sub-network is connected. In case a sub-network is not connected, the costs for the simulation of the sub-network are overestimated in Eq. (19) because each connected part can be treated separately since the matrix Y_{Ni} is

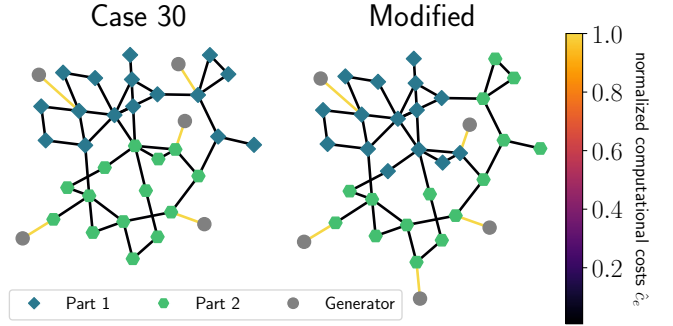


Fig. 2. Optimal partitionings for Case 30 (left) and a modified Case 30 (right), where one generator has been moved to a different bus. The optimal solutions have been obtained using Gurobi.

itself also a block matrix. Nevertheless, disconnected solutions are feasible solutions for distributed parallel simulation.

Ensuring connectedness is a similar problem to the traveling salesperson problem (TSP), where a satisfactory solution describes a *single* tour passing through all the cities that need to be visited. A known issue in the Dantzig-Fulkerson-Johnson formulation [49] of the TSP is that solutions often contain sub-tours, i.e., tours through subsets of cities. An approach for dealing with these disconnected sub-tours is the "finger-in-the-dike" method [50], where the problem is initially solved without banning sub-tours, and ad-hoc constraints are introduced iteratively to the original formulation to ban them as they appear in the sampled solutions. Analogously, here, one could ban disconnected sub-networks as they are sampled to ensure the connectedness of the sub-networks.

VI. RESULTS

For reproducibility and the fact that most readers will be familiar, we use the IEEE14, 30, 57, 89, 118, 145, 200, 300 [51] test grids to investigate optimal solutions, resource demands and solution quality on the QPU for $Q_{part.}$

A. Optimal Solutions

We use Gurobi to find the optimal solutions of $Q_{part.}$ for the test cases with 14, 30 and 57 buses. The MIP gap is set to 0.01. Obtaining the optimal solutions using a deterministic solver is necessary to evaluate the quality of the lowest energy states sampled by the D-Wave annealer.

The optimal solutions for a small test case demonstrate that minimizing $Q_{part.}$ gives a reasonable partition into two sub-networks, for example, cf. Fig. 2 for the 30-bus system. The sub-network sizes and the components are balanced and the cut sets are small. Furthermore, changes or modifications in the network, e.g., moving a generator, can lead to a different partitioning; see the right panel in Fig. 2. Changing the position of a generator is clear not a real life scenario but network reconfigurations are, a different optimal partitioning exists for each configuration. However, the partitioning itself introduces an overhead: $Q_{part.}$ has to be minimized, and LU decomposition has to be performed. Therefore, if a change is only persistent for a short time, re-partitioning may increase

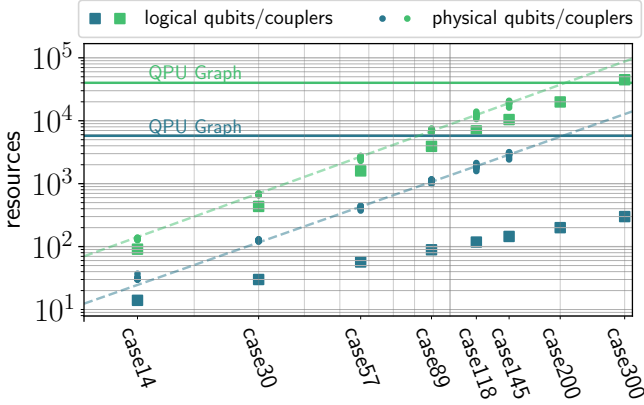


Fig. 3. Scaling of the number of logical (rectangles) and physical (circles) qubits (blue) and couplers (green) for the QUBO Q_{part} against the grid size of several IEEE test cases given by the number of buses. The physical resources can be estimated by power laws (dashed lines). The hardware limits are drawn as horizontal lines.

the overall computational cost of the simulation. In our future work, we plan to investigate whether we can include the overhead of repartitioning in the framework.

B. Scaling of Computational Resources

By construction, the number of logical variables $N_{q,log}$ is given by the number of buses N in the grid. $Q_{components}$ (21) and $Q_{network}$ (23) are fully connected QUBO objectives, i.e., each logical qubit has a nonvanishing coupling to every other logical qubit. Thus the full QUBO has $N_{c,log} = N^2/2$ logical interactions between logical qubits.

Since complete graphs, and thus fully connected QUBOs, can only be directly embedded for $N \leq 4$ on the D-Wave Advantage System 5.4 (JUPSI) with Pegasus topology [52], [53], the actual resources exceed the logical ones as we have to find minor embeddings for all test cases. We heuristically sample 10 minor embeddings for each test case to generate some minimal statistics. For the 200 and 300 bus test cases no embedding could be found in a reasonable time. For the smaller test cases, we find that the number of physical qubits $N_{q,phy}$ approximately follows a power law $N_{q,phy} \approx 0.11N^{2.04}$ in the number of logical qubits N . The power law scales similarly to the number of logical interactions $N_{c,log}$. Likewise, the number of physical couplers $N_{c,phy}$ needed to embed the problem follows a similar power law $N_{c,phy} \approx 0.56N_{c,log}^{2.09}$ in the number of logical interactions, see Fig. 3.

Both power laws estimate resources for other system sizes. The power laws suggest that the current hardware limits are reached at around 200 buses. This is consistent with our findings that no embeddings were found for 200 buses.

C. Dependence of Solution Quality on Annealing Hyperparameters

The quality of the sampled solution on the QPU depends strongly on the annealing hyperparameters. We evaluate the quality of a sample set by considering the time to the best

solution $TTS(5)$ for $p_S = 0.99$ together with the lowest relative error L_{min} (4) of the sample set. No optimal solution is obtained if $L_{min} > 0$. To generate robust statistics, the sample set for a hyperparameter configuration for case 14 consists of $N_s = 10^4$ samples, for case 30 and case 57 of $N_s = 10^5$ samples.

Similar to the observations made by Gonzalez Calaza et al. [54], we find that the solution quality is sensitive to the used embedding and the *chain strength* CS , that is, the coupling strength of the physical qubits in a chain, see Fig. 4. For this analysis, we set the annealing time to $T_A = 50\mu s$. Furthermore, for better comparison between the test cases, we consider the *relative chain strength* [54] given by

$$RCS = \frac{CS}{\max_{(n,m)} |(Q_{part})_{n,m}|}.$$

For case 14, the fastest TTS over all ten embeddings is given for RCS between 0.1 and 0.3; see the right panel in Fig. 4a. Each embedding is assigned a color for better comparison. The performance of the embeddings varies significantly, especially for small $RCS < 0.1$. The TTS roughly follows a convex function for all embeddings. If the chain strength is too small, the chains break regularly and thus do not uniquely represent a logical qubit. On the other hand, if the chain strength is too high, the dynamics during annealing are dominated by the internal dynamics of the chains.

For the best-performing embedding for each RCS , the optimal solution could be found over almost the whole range of chain strengths, except for one outlier, see the left panel of Fig. 4a. The outlier with $L_{min} > 0$ has a lower TTS , since the best sampled near-optimal solutions occur more frequently in the sample set than the optimal solutions for the other embeddings. For case 30, the TTS and L_{min} show similar behavior for the best embedding and chain strength combinations. The TTS follows a convex function in the RCS with a minimum between 0.02 and 0.1. However, the TTS is at least 10 times slower than for case 14. For case 57, the current hardware limits are reached, at least as a global optimal solver. No optimal solutions could be found for any embedding and chain strength. Additionally (not shown in the figure), we sampled the QPU 10^6 times for the best-performing combination of RCS and embedding for case 57, which did not significantly improve the solution quality.

Another hyperparameter that, by definition, affects the TTS is the annealing time T_A . For the best embedding and chain strength combinations from the previous analysis, the TTS monotonically increases in T_A for all three cases; see Fig. 4b. Here, we set $N_s = 10^5$ for all configurations. The smaller problems, which do not seem to need hyperparameter optimization, could profit from using the fast annealing feature, which just became available, to achieve an even smaller TTS .

Other hyperparameters, in particular anneal offsets, have also been found to be important for graph partitioning [55]. It has been demonstrated that tuning anneal offsets on a qubit level can prevent chains from freezing out early during the anneal [30] and to prevent perturbative anticrossings [32]. However, since tuning anneal offsets is quite resource-intensive, we leave this for future work.

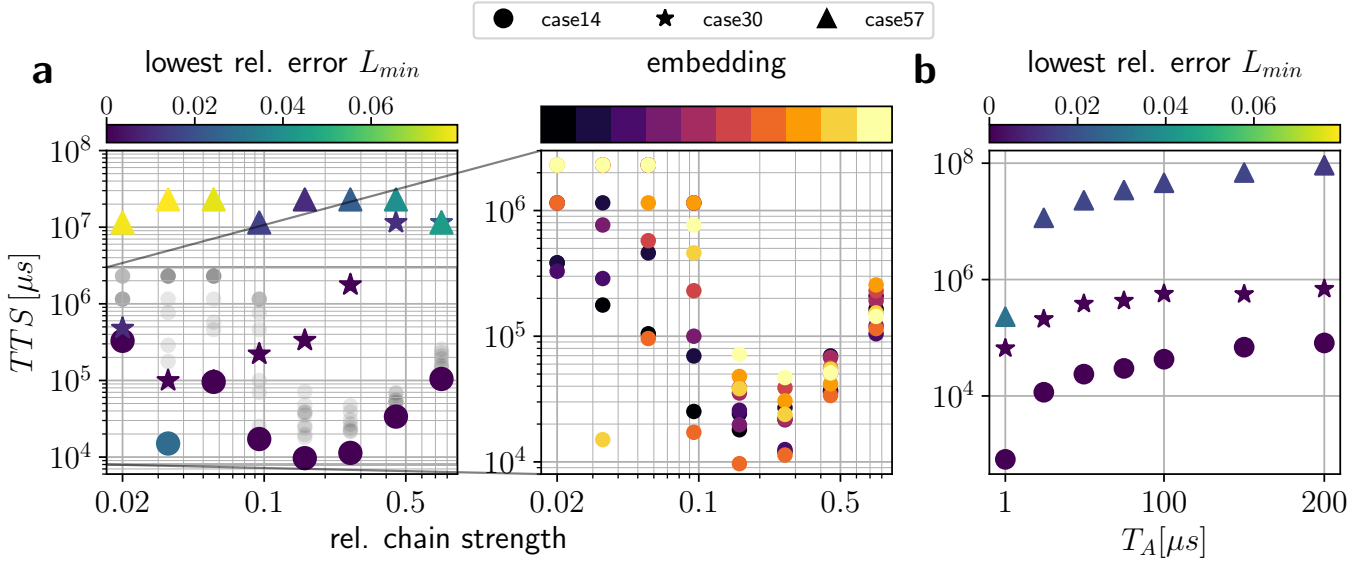


Fig. 4. Dependence of solution quality on quantum annealing hyperparameters. **a**: The left panel shows the dependence of the TTS for $p_S = 0.99$ and L_{min} on the RCS for only the best embeddings for cases 14, 30 and 57. For case 14, the right panel shows the variance in TTS between different embeddings (encoded by colors). **b**: Dependence of the TTS together with L on the annealing time T_A for the optimal embedding and chain strength combination found in **a**.

We conclude that the performance of QA depends strongly on hyperparameters, particularly on the embedding and the chain strength. Furthermore, for quantum annealing, the actual time to solution suffers from overheads, i. e. the time needed to embed the problem and network latency. For a fair comparison between the performances of quantum annealing on current prototypical hardware with classical deterministic or heuristic solvers, the overhead must be included, and the question arises whether to compare optimized solvers. A fair comparison would thus reveal current hardware limitations of the D-Wave machine, in particular, the need for minor embeddings [56], and is thus not meaningful for the future where some problems might have been overcome, e.g., by adapting the driver to expand the minimal gap [57]. In this work, we thus omit a benchmarking study and refer to the recent literature: For other highly connected Ising problems, quantum annealing on current D-Wave machines does not provide a speed up or better solution quality [56], [58], [59].

D. Near Optimal Solutions

For larger grids and using non-optimal hyperparameters, we are likely to only sample near-optimal solutions $L > 0$ on the QPU. For distributed parallel simulation, all partitionings are, in principle, feasible solutions. If the partitioning is done in the loop, the total runtime is the sum of the overhead due to optimizing the partitioning, i. e. determined by the number of samples N_s , the annealing time T_A , and the runtime of the distributed simulation. Instead of solving the grid partitioning QUBO (20) up to optimality, which for large grids becomes very hard, sampling near-optimal solutions very fast might be a viable near-term application of quantum annealing. The trade-off between shorter overheads due to sampling fewer solution candidates and longer simulation times due to sub-optimal

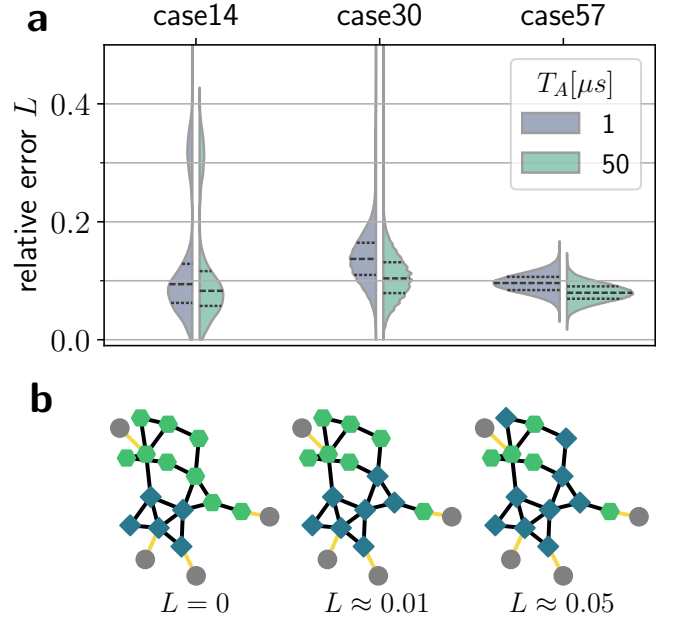


Fig. 5. Assessment of near-optimal solutions. **a**: Comparison of the distributions of L between different test cases and annealing times T_A . **b**: Near-optimal partitionings ($L > 0$) for the 14 bus test case in comparison to the optimal partitioning ($L = 0$).

partitionings needs to be investigated in a separate study. The optimal number of samples will also depend on how often we need to (re-)partition the network.

Furthermore, the optimal number of samples also depends on the annealing time T_A . As a preliminary step, we investigate the distribution of the relative error L for the best embedding and chain strength combinations found in the previous section for different T_A , cf. Fig. 5a. We find that the mean and the

quantiles of the distributions of L are, as expected, lower for $T_A = 50\mu s$ than for $T_A = 1\mu s$. Hence, the optimal T_A for the whole loop can not be assessed by just looking at the TTS for the optimization problem alone. The distributions of L also reveal that the variance in L becomes smaller for larger grids. More surprisingly, the mean of the distributions for case 57 is lower than for case 30. Hence, we can hope that sampling partitionings on current (or near-term) QPUs for larger grids will also return near-optimal solutions that are good enough to provide simulation speed-ups in competitive time.

Near-optimal solutions might be less intuitive than optimally partitioned sub-networks. For case 14, first, the cut becomes larger with increasing L ; however, the components and sub-network sizes remain (roughly) balanced, cf. Fig. 5b. The increase in cut size leads to disconnected sub-networks.

VII. CONCLUSION AND OUTLOOK

This article presents a novel quantum optimization approach to optimal grid partitioning for diakops-based parallel simulation approaches for power grids. We derived a QUBO formulation by mapping the problem-specific objectives, i.e. minimizing the idle times and the overhead due to the cut, to general QUBO objectives for graph partitioning; an approach that might be repeated for other grid partitioning applications [1], [3], [4]. The QUBO scales linearly in the number of buses and is thus efficient for optimal hardware. Moreover, the optimal solutions to the QUBO formulation provide reasonable partitionings for some small test cases.

Furthermore, for current quantum hardware, we have demonstrated that

- 1) the partitioning of only small grids can be optimized since the QUBOs connectivity requires an embedding on the QPU graph,
- 2) the TTS and the quality of the solutions depend on the grid size such that for a test case with 57 buses no optimal solution can be found in reasonable time, and
- 3) the TTS and the quality of the solutions are highly sensitive to annealing hyperparameters such as the embedding and the annealing time.

These problems are on such a fundamental level, that benchmarking the quantum solver against classical deterministic optimization approaches is, in our view, not meaningful. The current quantum annealers are too noisy and too sensitive to the choice of hyperparameters.

In our future research, we plan to investigate whether sampling near-optimal solution fast might be preferred over opting for optimal solutions to the QUBO when accounting for the whole partitioning-simulation loop. This is of interest, especially if network topologies change frequently. Whether QA might then offer an advantage over other heuristic approaches, c.f. [9], must be studied.

We are also planning to investigate whether it is sensible to formulate a more complicated objective function, e.g. to enforce connectivity of the sub-networks or to include modularity to limit solver iteration, hoping to achieve more optimal overall performance considering the partitioning together with the parallel simulation.

VIII. ACKNOWLEDGEMENTS

The paper was written as part of the project "Quantum-based Energy Grids (QuGrids)", which is receiving funding from the programme "Profilbildung 2022", an initiative of the Ministry of Culture and Science of the State of North Rhine-Westphalia. The authors gratefully acknowledge the Jülich Supercomputing Centre (<https://www.fz-juelich.de/en/ias/jsc/systems/supercomputers/apply-for-computing-time/juniq>) for funding this project by providing computing time on the D-Wave Advantage™ System JUPSI through the Jülich UNified Infrastructure for Quantum computing (JUNIQU), which has received funding from the German Federal Ministry of Education and Research (BMBF) and the Ministry of Culture and Science of the State of North Rhine-Westphalia. The authors also thank Manuel Dahmen for the fruitful discussions. The sole responsibility for the content of this publication lies with the authors.

REFERENCES

- [1] W. Jiang, V. Vittal, and G. T. Heydt, "Diakoptic state estimation using phasor measurement units," *IEEE Transactions on Power Systems*, vol. 23, no. 4, pp. 1580–1589, 2008.
- [2] R. J. Sánchez-García, M. Fennelly, S. Norris, N. Wright, G. Niblo, J. Brodzki, and J. W. Bialek, "Hierarchical spectral clustering of power grids," *IEEE Transactions on Power Systems*, vol. 29, no. 5, pp. 2229–2237, 2014.
- [3] E. Cotilla-Sanchez, P. D. H. Hines, C. Barrows, S. Blumsack, and M. Patel, "Multi-attribute partitioning of power networks based on electrical distance," *IEEE Transactions on Power Systems*, vol. 28, no. 4, pp. 4979–4987, 2013.
- [4] R. J. Sánchez-García, M. Fennelly, S. Norris, N. Wright, G. Niblo, J. Brodzki, and J. W. Bialek, "Hierarchical spectral clustering of power grids," *IEEE Transactions on Power Systems*, vol. 29, no. 5, pp. 2229–2237, 2014.
- [5] M. Armstrong, J. Marti, L. Linares, and P. Kundur, "Multilevel MATE for efficient simultaneous solution of control systems and nonlinearities in the OVNI simulator," *IEEE Transactions on Power Systems*, vol. 21, no. 3, pp. 1250–1259, Aug. 2006.
- [6] C. Dufour, J. Mahseredjian, and J. Bélanger, "A combined state-space nodal method for the simulation of power system transients," *IEEE Transactions on Power Delivery*, vol. 26, no. 2, pp. 928–935, Apr. 2011.
- [7] A. Benigni and A. Monti, "A parallel approach to real-time simulation of power electronics systems," *IEEE Transactions on Power Electronics*, vol. 30, no. 9, pp. 5192–5206, Sep. 2015.
- [8] R. Karp, "Reducibility among combinatorial problems," in *Complexity of Computer Computations*, R. Miller and J. Thatcher, Eds. Plenum Press, 1972, pp. 85–103.
- [9] M. Kyesswa, A. Murray, P. Schmurr, H. Çakmak, U. Kühnapfel, and V. Hagenmeyer, "Impact of grid partitioning algorithms on combined distributed ac optimal power flow and parallel dynamic power grid simulation," *IET Generation, Transmission & Distribution*, vol. 14, no. 25, pp. 6133–6141, 2020.
- [10] Y. Zhou, Z. Tang, N. Nikmehr, P. Babahajiani, F. Feng, T.-C. Wei, H. Zheng, and P. Zhang, "Quantum computing in power systems," *IEnergy*, vol. 1, no. 2, pp. 170–187, 2022.
- [11] T. Morstyn and X. Wang, "Opportunities for quantum computing within net-zero power system optimization," *Joule*, 2024.
- [12] A. W. Harrow, A. Hassidim, and S. Lloyd, "Quantum algorithm for linear systems of equations," *Physical review letters*, vol. 103, no. 15, p. 150502, 2009.
- [13] M. Cerezo, A. Arrasmith, R. Babbush, S. C. Benjamin, S. Endo, K. Fujii, J. R. McClean, K. Mitarai, X. Yuan, L. Cincio *et al.*, "Variational quantum algorithms," *Nature Reviews Physics*, vol. 3, no. 9, pp. 625–644, 2021.
- [14] A. M. Childs, R. Kothari, and R. D. Somma, "Quantum algorithm for systems of linear equations with exponentially improved dependence on precision," *SIAM Journal on Computing*, vol. 46, no. 6, pp. 1920–1950, 2017.

- [15] R. Eskandarpour, P. Gokhale, A. Khodaei, F. T. Chong, A. Passo, and S. Bahramirad, "Quantum computing for enhancing grid security," *IEEE Transactions on Power Systems*, vol. 35, no. 5, pp. 4135–4137, 2020.
- [16] F. Feng, Y. Zhou, and P. Zhang, "Quantum power flow," *IEEE Transactions on Power Systems*, vol. 36, no. 4, pp. 3810–3812, 2021.
- [17] Y. Zhou, P. Zhang, and F. Feng, "Noisy-intermediate-scale quantum electromagnetic transients program," *IEEE Transactions on Power Systems*, vol. 38, no. 2, pp. 1558–1571, 2022.
- [18] A. Ajagekar and F. You, "Quantum computing for energy systems optimization: Challenges and opportunities," *Energy*, vol. 179, pp. 76–89, 2019.
- [19] F. F. Silva, P. M. Carvalho, L. A. Ferreira, and Y. Omar, "A qubo formulation for minimum loss network reconfiguration," *IEEE Transactions on Power Systems*, vol. 38, no. 5, pp. 4559–4571, 2022.
- [20] T. Morstyn, "Annealing-based quantum computing for combinatorial optimal power flow," *IEEE Transactions on Smart Grid*, vol. 14, no. 2, pp. 1093–1102, 2022.
- [21] N. Nikmehr, P. Zhang, and M. A. Bragin, "Quantum distributed unit commitment: An application in microgrids," *IEEE transactions on power systems*, vol. 37, no. 5, pp. 3592–3603, 2022.
- [22] F. Feng, P. Zhang, M. A. Bragin, and Y. Zhou, "Novel resolution of unit commitment problems through quantum surrogate lagrangian relaxation," *IEEE Transactions on Power Systems*, vol. 38, no. 3, pp. 2460–2471, 2022.
- [23] N. G. Paterakis, "Hybrid quantum-classical multi-cut benders approach with a power system application," *Computers & Chemical Engineering*, vol. 172, p. 108161, 2023.
- [24] A. Lucas, "Ising formulations of many NP problems," *Frontiers in Physics*, vol. 2, 2014.
- [25] E. Farhi, J. Goldstone, S. Gutmann, and M. Sipser, "Quantum Computation by Adiabatic Evolution," Jan. 2000.
- [26] E. Farhi, J. Goldstone, and S. Gutmann, "A quantum approximate optimization algorithm," Nov. 2014.
- [27] D. Wang, K. Zheng, F. Teng, and Q. Chen, "Quantum Annealing With Integer Slack Variables for Grid Partitioning," *IEEE Transactions on Power Systems*, vol. 38, no. 2, pp. 1747–1750, Mar. 2023.
- [28] M. Born and V. Fock, "Beweis des Adiabatsatzes," *Zeitschrift für Physik*, vol. 51, no. 3, pp. 165–180, Mar. 1928.
- [29] T. Albash and D. A. Lidar, "Adiabatic quantum computation," *Reviews of Modern Physics*, vol. 90, no. 1, p. 015002, Jan. 2018.
- [30] E. Andriyash, Z. Bian, F. Chudak, M. Drew-Brook, A. D. King, W. G. Macready, and A. Roy, "Boosting Integer Factoring Performance via quantum annealing offsets," D-Wave Technical Report Series, Tech. Rep., Dec. 2016. [Online]. Available: https://www.dwavesys.com/media/10tjzis2/14-1002a_b_tr_boosting_integer_factorization_via_quantum_annealing_offsets.pdf
- [31] S. Jansen, M.-B. Ruskai, and R. Seiler, "Bounds for the adiabatic approximation with applications to quantum computation," *Journal of Mathematical Physics*, vol. 48, no. 10, p. 102111, Oct. 2007.
- [32] T. Lanting, A. D. King, B. Evert, and E. Hoskinson, "Experimental demonstration of perturbative anticrossing mitigation using nonuniform driver Hamiltonians," *Physical Review A*, vol. 96, no. 4, p. 042322, Oct. 2017.
- [33] T. Kadowaki and H. Nishimori, "Quantum annealing in the transverse Ising model," *Physical Review E*, vol. 58, no. 5, pp. 5355–5363, Nov. 1998, publisher: American Physical Society.
- [34] C. McGeoch and P. Farre, "The D-Wave Advantage System: An Overview," D-Wave, Tech. Rep., 2020. [Online]. Available: https://www.dwavesys.com/media/s3qbjp3s/14-1049a-a_the_d-wave_advantage_system_an_overview.pdf
- [35] C. C. McGeoch and P. Farre, "Milestones on the quantum utility highway," 2023.
- [36] "Operation and timing of D-wave quantum computers." [Online]. Available: https://docs.dwavesys.com/docs/latest/c_qpu_timing.html#qpu-timing-runtime-limits
- [37] V. Choi, "Minor-embedding in adiabatic quantum computation: I. The parameter setting problem," *Quantum Information Processing*, vol. 7, no. 5, pp. 193–209, Oct. 2008.
- [38] J. Cai, W. G. Macready, and A. Roy, "A practical heuristic for finding graph minors," Jun. 2014.
- [39] M. E. J. Newman, "Modularity and community structure in networks," *Proceedings of the National Academy of Sciences*, vol. 103, no. 23, p. 8577–8582, Jun. 2006.
- [40] Y. Chen, G. Paul, S. Havlin, F. Liljeros, and H. E. Stanley, "Finding a better immunization strategy," *Phys. Rev. Lett.*, vol. 101, p. 058701, Jul 2008.
- [41] A. Billionnet and B. Jaumard, "A decomposition method for minimizing quadratic pseudo-boolean functions," *Oper. Res. Lett.*, vol. 8, no. 3, p. 161–163, jun 1989.
- [42] A. Buluç, H. Meyerhenke, I. Safro, P. Sanders, and C. Schulz, *Recent Advances in Graph Partitioning*. Cham: Springer International Publishing, 2016, pp. 117–158.
- [43] L. R. Ford and D. R. Fulkerson, "Maximal flow through a network," *Canadian Journal of Mathematics*, vol. 8, p. 399–404, 1956.
- [44] I. Das and J. E. Dennis, "A closer look at drawbacks of minimizing weighted sums of objectives for Pareto set generation in multicriteria optimization problems," *Structural optimization*, vol. 14, no. 1, pp. 63–69, Aug. 1997.
- [45] H. Happ, "Diakoptics—The solution of system problems by tearing," *Proceedings of the IEEE*, vol. 62, no. 7, pp. 930–940, Jul. 1974.
- [46] J. Shu, W. Xue, and W. Zheng, "A Parallel Transient Stability Simulation for Power Systems," *IEEE Transactions on Power Systems*, vol. 20, no. 4, pp. 1709–1717, Nov. 2005.
- [47] J. Zhang, M. Mittenbühler, and A. Benigni, "Shifted frequency analysis based, faster-than-real-time simulation of power systems on graphics processing unit," *International Journal of Electrical Power & Energy Systems*, vol. 159, p. 110014, Aug. 2024.
- [48] P. Aristidou, D. Fabozzi, and T. Van Cutsem, "Dynamic simulation of large-scale power systems using a parallel schur-complement-based decomposition method," *IEEE Transactions on Parallel and Distributed Systems*, vol. 25, no. 10, pp. 2561–2570, Oct. 2014.
- [49] G. B. Dantzig, D. R. Fulkerson, and S. M. Johnson, *Solution of a Large-Scale Traveling-Salesman Problem*. Santa Monica, CA: RAND Corporation, 1954.
- [50] J. A. Montañez-Barrera, P. van den Heuvel, D. Willsch, and K. Michielsen, "Improving performance in combinatorial optimization problems with inequality constraints: An evaluation of the unbalanced penalization method on d-wave advantage," in *2023 IEEE International Conference on Quantum Computing and Engineering (QCE)*. IEEE, Sep. 2023.
- [51] "Example Matpower Cases." [Online]. Available: <https://matpower.app/manual/matpower/ExamplematpowerCases.html>
- [52] J. R. Kelly Boothby, Paul Bunyk and A. Roy, "Next-Generation Topology of D-Wave Quantum Processors," D-Wave Technical Report Series, Tech. Rep., 2019. [Online]. Available: https://www.dwavesys.com/media/jwwj5z3z/14-1026a-c_next-generation-topology-of-dw-quantum-processors.pdf
- [53] C. McGeoch and P. Farré, "Advantage Processor Overview," D-Wave Technical Report Series, Tech. Rep., 2022. [Online]. Available: https://www.dwavesys.com/media/3xvdipec/14-1058a-a_advantage_processor_overview.pdf
- [54] C. D. Gonzalez Calaza, D. Willsch, and K. Michielsen, "Garden optimization problems for benchmarking quantum annealers," *Quantum Information Processing*, vol. 20, no. 9, p. 305, Sep. 2021.
- [55] A. Barbosa, E. Pelofske, G. Hahn, and H. N. Djidjev, "Optimizing embedding-related quantum annealing parameters for reducing hardware bias," 2021, pp. 162–173.
- [56] D. Vert, M. Willsch, B. Yenilen, R. Sirdey, S. Louise, and K. Michielsen, "Benchmarking quantum annealing with maximum cardinality matching problems," *Frontiers in Computer Science*, vol. 6, p. 1286057, 2024.
- [57] I. Hen and F. M. Spedalieri, "Quantum Annealing for Constrained Optimization," *Physical Review Applied*, vol. 5, no. 3, p. 034007, Mar. 2016.
- [58] R. Au-Yeung, N. Chancellor, and P. Halfmann, "Np-hard but no longer hard to solve? using quantum computing to tackle optimization problems," *Frontiers in Quantum Science and Technology*, vol. 2, p. 1128576, 2023.
- [59] N. Mohseni, P. L. McMahon, and T. Byrnes, "Ising machines as hardware solvers of combinatorial optimization problems," *Nature Reviews Physics*, vol. 4, no. 6, pp. 363–379, 2022.